JMEPEG (2013) 22:405–409
DOI: 10.1007/s11665-012-0289-x

1059-9495/$19.00

Highly Porous NiTi with Isotropic Pore Morphology Fabricated by Self-Propagated High-Temperature Synthesis

S.A. Hosseini, M. Alizadeh, A. Ghasemi, and M.A. Meshkot

(Submitted February 16, 2012; in revised form May 28, 2012; published online July 10, 2012)

Highly porous NiTi with isotropic pore morphology has been successfully produced by self-propagating high-temperature synthesis of elemental Ni/Ti metallic powders. The effects of adding urea and NaCl as temporary pore fillers were investigated on pore morphology, microstructure, chemical composition, and the phase transformation temperatures of specimens. These parameters were studied by optical microscopy, scanning electron microscopy, x-ray diffraction, and differential scanning calorimetry (DSC). Highly porous specimens were obtained with up to 83% total porosity and pore sizes between 300 and 500 μm in diameter. Results show pore characteristics were improved from anisotropic to isotropic and pore morphology was changed from channel-like to irregular by adding pore filler powders. Furthermore, the highly porous specimens produced when using urea as a space holder, were of more uniform composition in comparison to NaCl. DSC results showed that a two-step martensitic phase transformation takes place during the cooling cycles and the austenite finish temperature (A_f) is close to human body temperature. Compression test results reveal that the compressive strength of highly porous NiTi is about 155 MPa and recoverable strain about 6% in superelasticity regime.

Keywords Highly porous NiTi, Pore characteristics, SHS, Space holder

1. Introduction

Porous metallic biomaterials, such as NiTi, are good candidates for load-bearing biological implant applications. Researchers have focused on porous biomaterials due to their adjustable mechanical properties and capacity for tissue in-growth into their porous structure. Tissue in-growth results in strong fixation of human implants (Ref 1-4). Previous researches confirm the preference of NiTi alloys for their mechanical properties as compared to other biomaterials. In addition, the combination of other properties such as superelasticity, shape memory effect, and excellent biocompatibility, makes NiTi alloys most suitable for hard tissue replacement (Ref 3-7).

Various metallurgical methods may be used to produce porous NiTi parts, e.g., conventional sintering, self-propagating high-temperature synthesis (SHS), hot isostatic pressing (HIP), metal injection molding (MIM), and spark plasma sintering (SPS) (Ref 5-9). Among these methods, SHS is a more acceptable technique due to time and energy saving.

In the SHS method, elemental powders of Ni and Ti are cold pressed into the desired shape and then ignited by a local ignition source such as a tungsten coil, laser beam, microwave, etc. (Ref 10-12). An exothermic reaction starts at the ignition point which supplies the activation energy for the remaining parts of the specimen. In this way, a combustion wave of the exothermic reaction is propagated through the green compacted specimen. A preheating step before the ignition is generally necessary due to the relatively low heat of the reaction between elemental nickel and titanium powders (Ref 2).

Undesirable pore morphology is one disadvantage of specimens produced by the SHS method. After synthesis, most pores are found to be elongated perpendicular to the propagating direction. Porous NiTi parts with 30-70% porosity have been achieved by this method (Ref 6, 10-17). Several parameters such as preheating temperature, green state porosity, heating rate, and compaction pressure influence the final pore characteristics, microstructure, and mechanical properties of porous NiTi obtained through SHS. It has been reported that final porosity was increased with increasing green state porosity and decreasing preheating temperature (Ref 13-17). Tay et al. (Ref 13) reported green porosity to be the main source of total porosity. As porosity of the green state decreases, e.g., by increased compaction pressure, the final porosity of specimens decreases and subsequently, mechanical properties will be improved (Ref 14). In addition, Li et al. (Ref 15) reported higher preheating temperature causes an anisotropic pore morphology. At the same time, specimens with a higher green density have a more homogeneous microstructure (Ref 16).

Recently, using space holder materials is claimed to be a successful method to improve pore characteristics of highly porous NiTi (Ref 2, 18). Urea, NaCl, and ammonium carbonate have been used as conventional space holders. In this research, the pore characteristics and microstructure and mechanical properties of porous NiTi produced by SHS were investigated after adding different amounts of space holder.

S.A. Hosseini, M. Alizadeh, A. Ghasemi, and **M.A. Meshkot**, Materials and Energy Research Center, P.O. Box 14155-4777, Tehran, Iran. Contact e-mail: mehdializadeh@merc.ac.ir.

2. Methods and Materials

Elemental nickel (>10 μm) and titanium (>44 μm) powders with urea and NaCl as temporary space holder powders were used for the fabrication of highly porous NiTi. Space holder powders were of 300 to 500 μm particles size. Powder mixtures of Ni and Ti containing 50.8at.%Ni-49.2at.%Ti and different volume percentage of temporary space holder powders, were mixed in a cylindrical ball mill at a speed of 400 rpm for 1 h to produce a homogenous mixture. The blended powders were compacted into cylindrical tablets at 200 MPa using a hydraulic press. To remove the NaCl temporary space holder, the green compacts were placed in distilled water for 24 h before synthesis. Then, all tablets were preheated at 300 °C for 1 h at a rate of 20 °C/min under a vacuum of 2×10^{-5} torr. Removal of urea occurred during the preheating treatment. In the next step a coil of tungsten wire was heated with a potential of 80 V to initiate the self-propagating combustion of the tablets. After combustion, some specimens were aged at 500 °C for 30 min.

Porosity of specimens was calculated by the Archimedes method in accordance with the following equations:

$$P_t = 100\left(1 - \frac{D_b}{D_t}\right) \quad \text{(Eq 1)}$$

$$D_b = \frac{W_a}{W_e - W_b} \times D_1 \quad \text{(Eq 2)}$$

where P_t is total porosity, D_t true density of NiTi, D_b density of porous NiTi that is determined by Eq 2. In this equation, W_a is the weight of dry specimens, W_e weight of specimens soaked and suspended in water, W_b weight of specimens soaked in water and suspended in air, and D_1 is the density of water at room temperature. Table 1 lists specimens with different volume percent of space holder and final porosity.

Phase structure analysis of specimens was carried out by x-ray diffraction (XRD) with Cu K_α radiation (λ = 1.54 Å) and diffraction angle in the range of 30°-90° with a step size of 0.020°. Scanning electron microscopy (SEM) and optical microscopy were used to show morphology, shape, size, and distribution of pores in the specimens.

Differential scanning calorimetry (DSC) was performed in the temperature range −50-100 °C with a heating and cooling rate of 10 °C/min to study phase transformation temperatures.

Cyclic compression tests were performed to evaluate mechanical properties and superelasticity of specimens using strains of 2, 4, 6, 8, 10, 15, 20, 30, 40, and 50%. The strain rate of compression tests were 0.5 mm/min and the test temperature was 36 ± 2 °C.

Table 1 Pore characteristics of specimens with different space holder (urea) amount

Designation	Urea, vol.%	Open porosity, %	Close porosity, %	Total porosity, %	Open pore ratio, %
S1	0	27	15	42	64
S2	15	41	18	59	69
S3	30	56	24	70	80
S4	45	73	10	83	88

3. Results and Discussion

3.1 Pore Morphology and Characteristics

Table 1 shows the amount of porosity in the specimens with different volume percent of space holder urea. The results show specimens with higher porosity are obtained by increasing the amount of space holder. According to Table 1, the porosity of the specimen without space holder is about 42%. Maximum porosity was obtained at about 83% with urea at 45 vol.% (Fig. 1).

As shown in Fig. 2, closed porosity was almost constant with varying amounts of urea. On the other hand, open porosity and the open to closed pore volume ratio was directly proportional to the amount of space holder. As a result, increasing total porosity is due only to an increase in open porosity.

Figure 3(a) illustrates macrograph of NiTi porous specimen synthesized by SHS without space holder. It shows most of the pores are larger than 500 μm. They are isolated and rarely interconnected. Also, the specimen with 15% urea has similar over-extended and channel-like pores oriented perpendicular to the combustion wave (Fig. 3b); albeit, the pore orientation depends on the point of ignition (Ref 19). The same results were reported by other researchers (Ref 13, 14, 19, 20). It seems some transient liquid phases are created due to locally high temperatures at the combustion front. As a result of a high-temperature gradient along the combustion wave, transient liquid phases are extended perpendicular to the combustion wave resulting in elongated pores. Previous researchers have shown that increasing the thermal energy of the specimen, e.g., by increasing the preheat temperature, intensifies this behavior

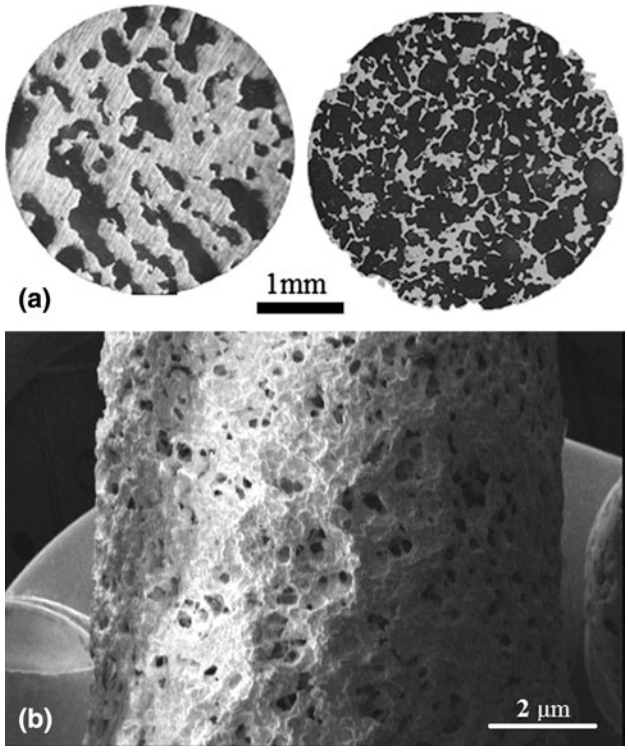

Fig. 1 (a) Comparison of optical micrograph of NiTi specimens with (right) and without space holder (left). (b) SEM micrograph of the specimen with 45% urea as space holder and 83% final porosity

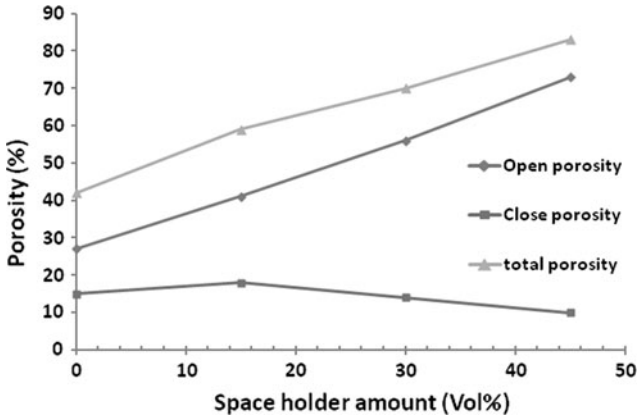

Fig. 2 Porosity percent vs. space holder (urea) amount in the porous NiTi specimens produced by SHS

(Ref 15). According to the work of Kaya et al. (Ref 20), mechanical properties depend on the orientation of combustion channels and minimum compressive strength for porous NiTi specimens is obtained when loading direction is perpendicular to the channels. Such elongated pores are considered to be inappropriate for orthopedic applications due to a lack of interconnectivity between elongated channels which may prohibit tissue in-growth.

Results show that channel-like pores gradually disappeared with increasing amount of space holder. As shown in Fig. 3(c), extended pores disappeared for the specimen with 45% space holder. The pores in this specimen are almost entirely isotropic and homogenously distributed. This structure results from reduced thermal energy which is due to a reduction of combustible materials per unit volume.

3.2 Microstructure of Porous Specimens

Figure 4(a)-(c) shows XRD patterns of the porous NiTi with and without space holder. The NiTi phase is dominant in the specimen without space holder (Fig. 4a).

For the specimen with urea space holder, still the NiTi phase is dominant, but peaks for other intermetallic phases such as Ti_2Ni and Ni_3Ti are detectable in the x-ray pattern. It seems that incomplete removal of the space holder and residual material causes the formation of other compounds. Pure Ni, Ti_2Ni, Ni_3Ti, and Ni_4Ti_3 phases present in SHS-produced NiTi increases the brittleness of the product. Moreover, if the mixing process is not uniform, more of the undesirable phases are produced (Ref 21). These phases could be eliminated by solution annealing and treatment under load (Ref 21). Also, NiTi yield increases with increasing preheat temperature (Ref 21).

Undesirable phases such as Ti_2Ni and Ni_3Ti were also formed in specimens with NaCl space holder. Residual NaCl reacts with the elemental powders and thereby hinders NiTi phase formation.

3.3 Phase Transformation Behavior

Figure 5(a) and (b) shows DSC cooling and heating curves of the porous NiTi specimens synthesized by SHS method, respectively. Before aging, the specimen did not show any heat flow peaks during cooling and heating on DSC curves. Similar behavior was detected in specimens that were produced by conventional sintering in our previous studies (Ref 22). Faults

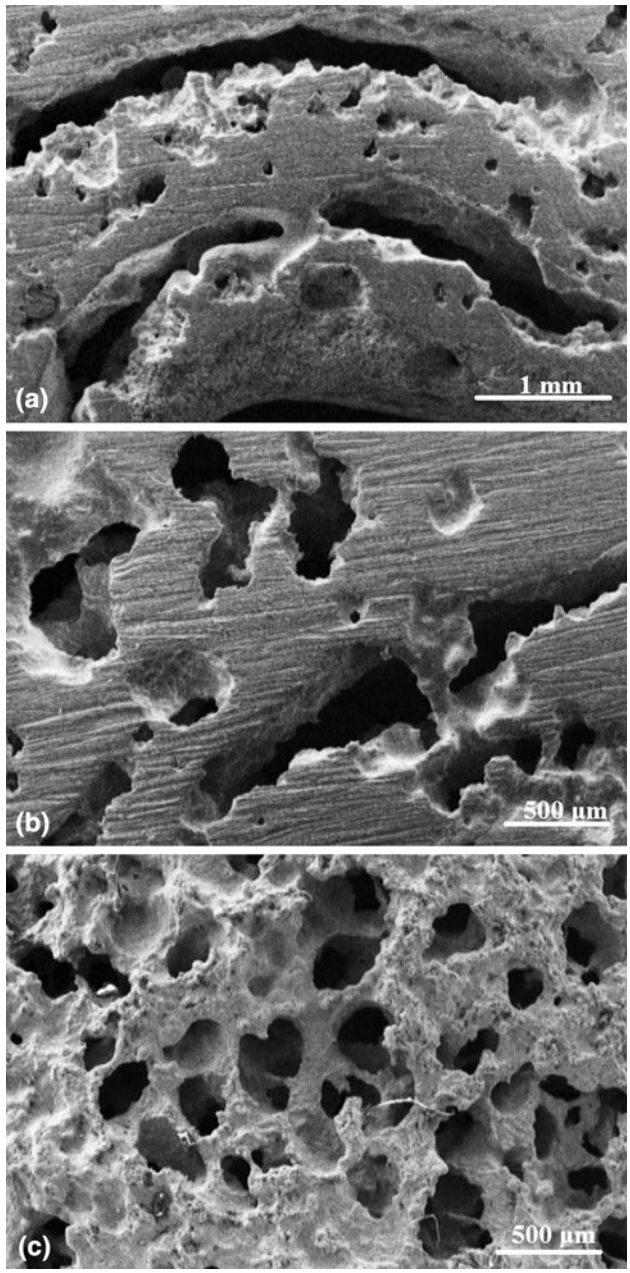

Fig. 3 SEM micrograph of porous specimens with different amount of urea space holder: (a) 0 vol.%, (b) 15 vol.%, (c) 45 vol.%

and defects in microstructure prevent transformations occurring at expected temperatures (Ref 22). When the porous NiTi specimens were heat treated at 500 °C for half an hour, two distinct peaks appeared in the DSC cooling curve. The first peak is related to austenite (A) to rhombohedral (R) transformation. The R phase is an intermediate phase that usually appears in Ni-rich NiTi alloys after aging treatment at 400-500 °C due to the formation of precipitates such as Ni_4Ti_3. The other peak corresponds to the transformation from R to martensite (M) phase during the cooling cycle.

The phase transformation temperatures of the specimen with 30% urea were found to be slightly higher than that without space holder (Table 2). The end of transformation temperature for austenite (A_f) is an important factor in the design of superelastic nitinol implants. Porous NiTi Specimens show

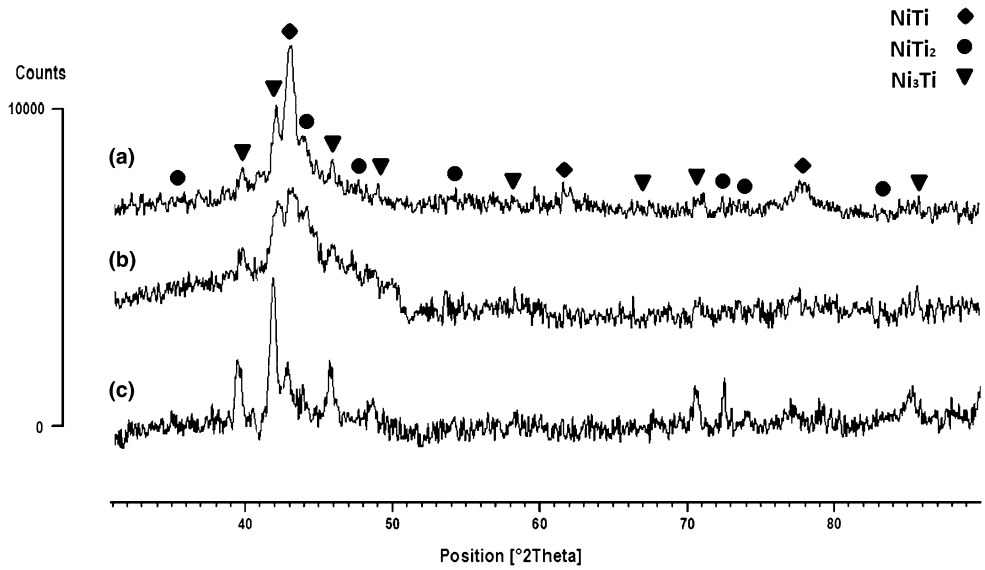

Fig. 4 XRD patterns of porous NiTi synthesized by SHS with different space holder material: (a) without space holder, (b) 45 vol.% urea, (c) 45 vol.% NaCl

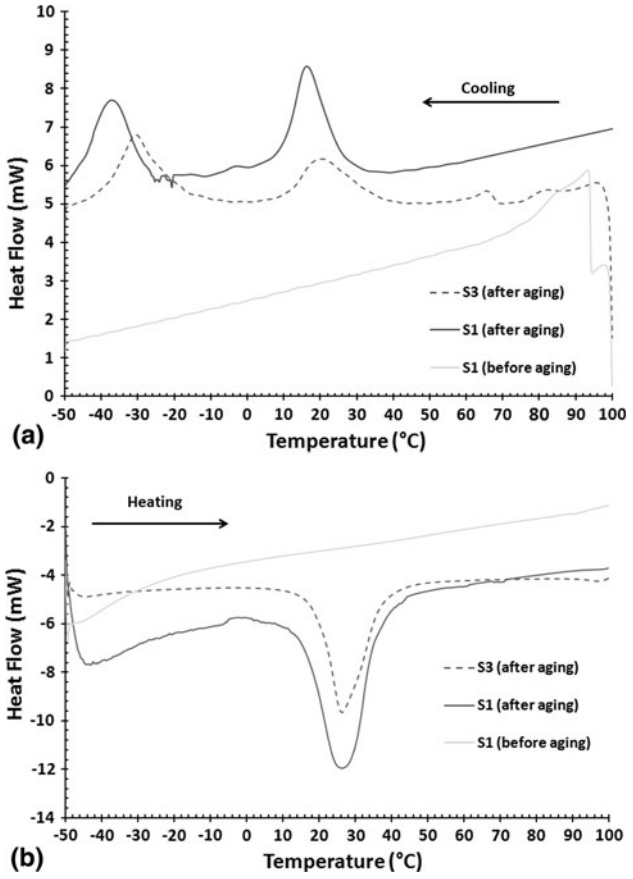

Fig. 5 (a) DSC cooling and (b) heating curves of the porous NiTi specimens with different amounts of space holder after heat treatment at 500 °C for half an hour

good superelasticity behavior when working temperature is near and slightly higher than A_f (Ref 2). The A_f of our specimens is close to body temperature (37 °C) which means they are suitable for biomedical applications.

Table 2 Phase transformation temperatures of porous NiTi produced by SHS (S1: without space holder, S3: with 30% urea)

Specimen no.	M_f	M_p	M_s	R_f	R_p	R_s	A_s	A_p	A_f
S1 (aged)	−48	−37	−28	10	16	27	15	26	36
S3 (aged)	−41	−31	−15	11	20	39	18	27	38

A, martensite to austenite transformation temperature; R, austenite to R phase transformation temperature; M, R phase to martensite transformation temperature; s, start point; p, peak point; f, finish point

3.4 Mechanical Properties of Highly Porous Specimen

As shown in Fig. 6, even after 50% strain, a typical specimen with 83% porosity has not failed. The maximum compressive strength of specimens was found to be 155 MPa which is very similar to that of human bones (between 100 and 200 MPa in compression mode (Ref 23)). Also, the experimental results show a mechanical hysteresis with 6% recoverable strain which proves superelastic behavior is exhibited even in highly porous specimens.

4. Conclusion

Highly porous NiTi specimens were produced with isotropic structure by SHS. Space holder's urea and NaCl were used to improve pore characteristics of porous NiTi. After the addition of space a holder, isolated channel-like pores were converted to isotropic interconnected pores, making the material suitable for biomedical applications. Highly porous NiTi with 83% porosity was obtained after the addition of 45 vol.% urea. Results show that urea is a better space holder material than NaCl for producing homogenous porous NiTi. DSC results showed that adding space holder has little effect on phase transformation temperatures. Further, the austenite phase has a stable

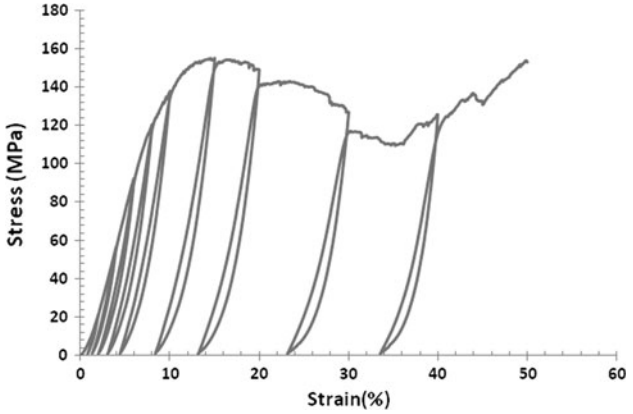

Fig. 6 Compressive test result typical of highly porous specimens with 83% porosity fabricated by SHS

microstructure at human body temperature which makes this material suitable for biomedical applications. Mechanical properties of the specimens are similar to bone with compressive strength of about 155 MPa and superelastic recoverable strain of 6%.

References

1. L.P. Lefebvre, J. Banhart, and D. Dunand, Porous Metals and Metallic Foams: Current Status and Recent Developments, *Adv. Eng. Mater.*, 2008, **10**(9), p 775–787
2. A. Bansiddhi, T.D. Sargeant, S.I. Stupp, and D.C. Dunand, Porous NiTi for Bone Implant: A Review, *Acta Biomater.*, 2008, **4**, p 773–782
3. M. Assad, F. Likibi, P. Jarzem, M.A. Leroux, C. Coillard, and C.H. Rivard, Porous Nitinol vs. Titanium Intervertebral Fusion Implants: Computer Tomography, Radiological and Histological Study of Osseointegration Capacity, *Mat.-Wiss. u. Werkstofftech.*, 2004, **35**, p 219–223
4. F. Likibi, M. Assad, C. Coillard, G. Chabot, and C.H. Rivard, Influence of Biomaterial Structure and Hardness on Its Osseo-integration: Histomorphometric Evaluation of Porous Nitinol and Titanium Implants, *Eur. J. Orthop. Surg. Traumatol.*, 2005, **15**, p 255–256
5. S.K. Sadrnezhaad and S.A. Hosseini, Fabrication of Porous NiTi-Shape Memory Alloy Objects by Partially Hydride Titanium Powder for Biomedical Applications, *Mater. Des.*, 2009, **30**, p 4483–4487
6. C.L. Chu, C.Y. Chung, P.H. Lin, and S.D. Wang, Fabrication of Porous NiTi Shape Memory Alloy for Hard Tissue Implants by Combustion Synthesis, *Mater. Sci. Eng., A*, 2004, **366**, p 114–119
7. C. Greiner, S.M. Oppenheimer, and D.C. Dunand, High Strength, low Stiffness, Porous NiTi with Superelastic Properties, *Acta Biomater.*, 2005, **1**, p 705–716
8. Y. Zhao, M. Taya, Y. Kang, and A. Kawasaki, Compression Behavior of Porous NiTi Shape Memory Alloy, *Acta Mater.*, 2005, **53**, p 337–343
9. M. Kohl, M. Bram, P. Buchkremer, D. Stover, T. Habijan, and M. Koller, Production of Highly Porous Near-Net-Shape NiTi Components for Biomedical Applications, *Metfoam Conference*, 2007
10. C.L. Yeh and W.Y. Sung, Synthesis of NiTi Intermetallics by Self-Propagating Combustion, *J. Alloys Compd.*, 2004, **376**(1–2), p 79–88
11. C. Zanotti, P. Giuliani, A. Terrosua, S. Gennari, and F. Maglia, Porous Ni-Ti Ignition and Combustion Synthesis, *Intermetallics*, 2007, **15**(3), p 404–412
12. I. Ganesh, R. Johnson, G.V.N. Rao, Y.R. Mahajana, S.S. Madavendr, and B.M. Reddy, Microwave-Assisted Combustion Synthesis of Nanocrystalline $MgAl_2O_4$ Spinel Powder, *Ceram. Int.*, 2005, **31**(1), p 67–74
13. B.Y. Tay, C.W. Goh, Y.W. Gu, C.S. Lim, M.S. Yong, M.K. Ho, and M.H. Myint, Porous NiTi Fabricated by Self-Propagating High-Temperature Synthesis of Elemental Powders, *J. Mater. Process. Technol.*, 2008, **202**, p 359–364
14. S.N. Denmud and L. Sikong, Characteristics and Compressive Properties of Porous NiTi Alloy Synthesized by SHS Technique, *Mater. Sci. Eng., A*, 2009, **515**, p 93–97
15. Y.H. Li, L.J. Rong, and Y.Y. Li, Pore Characteristics of Porous NiTi Alloy Fabricated by Combustion Synthesis, *J. Alloys Compd.*, 2001, **325**, p 259–262
16. G. Tosuna, L. Ozler, M. Kaya, and N. Orhan, A Study on Microstructure and Porosity of NiTi Alloy Implants Produced by SHS, *J. Alloys Compd.*, 2009, **487**, p 605–611
17. C.L. Chu, C.Y. Chung, P.H. Lin, and S.D. Wang, Fabrication and Properties of Porous NiTi Shape Memory Alloys for Heavy Load-Bearing Medical Applications, *J. Mater. Process. Technol.*, 2005, **169**, p 103–107
18. A. Bansiddhi and D. Dunand, Shape-Memory NiTi Foams Produced by Solid-State Replication with NaF, *Intermetallics*, 2007, **15**, p 1612–1622
19. M. Kaya, N. Orhan, and G. Tosun, Phase Transformation Behaviors of Porous NiTi SMA Fabricated as Hollow and Solid Cylinders by SHS, *Mater. Sci. Technol.*, 2010, **26**, p 522–527
20. M. Kaya, N. Orhan, and G. Tosun, The Effect of the Combustion Channels on the Compressive Strength of Porous NiTi Shape Memory Alloy Fabricated by SHS as Implant Material, *Curr. Opin. Solid State Mater. Sci.*, 2010, **14**, p 21–25
21. M. Kaya, N. Orhan, and B. Kurt, Effect of Solution Treatment Under Load on Microstructure and Fabrication of Porous NiTi Shape Memory Alloy by Self-Propagating High Temperature Synthesis, *Powder Metall.*, 2009, **52**, p 36–41
22. S.A. Hosseini, S.K. Sadrnezhaad, and A. Ekrami, Phase Transformation Behavior of Porous NiTi Alloy Fabricated by Powder Metallurgical Method, *Mater. Sci. Eng., C*, 2009, **29**, p 2203–2207
23. D.L. Wise, *Biocompatibility of Self-Reinforced Poly(lactide-co-glycolide) Implants, Biomaterials and Bioengineering Handbook*, 1st ed., CRC Press, Boca Raton, 2000, p 625